Current Biology 21, 1450–1459, September 13, 2011 ©2011 Elsevier Ltd All rights reserved DOI 10.1016/j.cub.2011.07.046

Article

Distinct Roles for F-BAR Proteins Cdc15p and Bzz1p in Actin Polymerization at Sites of Endocytosis in Fission Yeast

Rajesh Arasada[1] and Thomas D. Pollard[1,2,*]
[1]Department of Molecular,
Cellular and Developmental Biology
[2]Department of Cell Biology and Department of Molecular
Biophysics and Biochemistry
Yale University, PO Box 208103, New Haven,
CT 06520-8103, USA

Summary

Background: Genetic analyses of budding and fission yeast identified >50 proteins that assemble at sites of clathrin-mediated endocytosis in structures called actin patches. These proteins include clathrin, clathrin-interacting proteins, actin binding proteins, and peripheral membrane proteins such as F-BAR proteins. Many questions remain regarding the interactions of these proteins, particularly the participation of F-BAR proteins in the assembly of actin filaments.

Results: Our microscopic and genetic interaction experiments on fission yeast show that F-BAR proteins Cdc15p and Bzz1p accumulate in two distinct zones on invaginating membrane tubules and interact with Myo1p and Wsp1p, nucleation-promoting factors for Arp2/3 complex. The two F-BAR proteins peak prior to movement of the actin patch and their accumulation in actin patches depends on the nucleation-promoting factors. At their peak local concentrations, we estimated the stoichiometries of the proteins in actin patches to be one Bzz1p per two Wsp1p and one Cdc15p per Myo1p. Purified Bzz1p has two SH3 domains that interact with Wsp1p and stimulate actin polymerization by Arp2/3 complex. Cells lacking either Cdc15p or Bzz1p assemble 3- to 5-fold less actin in patches (in spite of normal levels of Wsp1p, Myo1p, and Arp2/3 complex), and patches move shorter distances from the plasma membrane.

Conclusion: We propose that during clathrin-mediated endocytosis, F-BAR proteins interact with nucleation-promoting factors to stimulate Arp2/3 complex in two different zones along the invaginating tubule. We further propose that polymerization of actin filaments in these two zones contributes to membrane scission.

Introduction

Cells use endocytosis to take up nutrients and internalize cell surface molecules. Yeasts rely mainly on clathrin-dependent mechanisms for endocytosis, whereas animal cells also use other mechanisms [1–4]. Clathrin-mediated endocytosis involves recruitment of proteins to a site where the plasma membrane invaginates and pinches off a vesicle. Fluorescence microscopy documented the time course of assembly of many of these proteins in yeast [5].

In mammalian cells, scission of an endocytic vesicle depends on the GTPase dynamin, which accumulates at the neck of the membrane invagination [6]. Budding and fission yeast encode three dynamin homologs, but none localize in actin patches [5]. Some studies showed that the budding yeast dynamin homolog Vps1p interacts with Sla1p and that *Δvps1* mutants accumulate depolarized actin aggregates and fail to internalize membrane receptors [7, 8]. Other studies reported that deletion of Vps1p did not affect endocytosis or the ultrastructure of actin patches in budding yeast [5, 9] or fission yeast [10].

Both yeasts depend on actin polymerization to generate tubular invaginations of the plasma membrane at sites of endocytosis [9]. Actin assembly is also important in clathrin-dependent, caveolin-dependent, and clathrin- and caveolin-independent endocytosis in animal cells [1, 11–15]. Mammalian cells use the same proteins to make both small clathrin-coated pits independent of the actin cytoskeleton and larger clathrin-coated plaques that require actin cytoskeleton [16]. In all carefully studied systems, actin assembly during endocytosis depends on Arp2/3 complex and its nucleation-promoting factors [5, 13, 17–19].

Some early endocytic proteins such as Pan1, Sla2, Hip1, Hip1R, proteins of the BAR superfamily (amphiphysin, SNX9, Toca1, Cip4, and FBP17), and dynamin associate with both membrane lipids and components of the actin cytoskeleton. These interactions link the plasma membrane and the actin cytoskeleton [6, 20–22], but the connections between actin polymerization and membrane reorganization are less well understood than actin assembly.

We used quantitative fluorescence microscopy to study the roles of F-BAR proteins Bzz1p and Cdc15p during endocytosis in fission yeast. Mutations in the *bzz1⁺* gene or depletion of Cdc15p impaired endocytosis and assembly of actin filaments in patches in spite of normal accumulation of WASp (Wsp1p), myosin-I (Myo1p), and Arp2/3 complex. Cdc15p assembled stoichiometrically with Myo1p, whereas Bzz1p assembled stoichiometrically with and activated Wsp1p. These features, as well as genetic interactions, lead us to propose that these two F-BAR proteins set up separate zones of actin assembly on tubular necks connecting coated pits to the surface membrane.

Results

F-BAR Proteins of *Schizosaccharomyces pombe*

The *Schizosaccharomyces pombe* genome contains seven genes encoding F-BAR domains (see also Figure S1 available online), a domain highly conserved from amoebas to mammals in the "pombe Cdc15 homology" (PCH) family of proteins. Previous work characterized six *S. pombe* F-BAR proteins, Cdc15p [23], Bzz1p [24], Imp2p [25], Rga7p [26–28], Rga8p [29], and Rga9p [29]. Open reading frame (ORF) SPBC12C2.05c *bzz1⁺* [24] groups with *Saccharomyces cerevisiae bzz1* [30] on a phylogenetic tree of F-BAR domains (Figure S1A). Uncharacterized *S. pombe* ORF SPBC4C3.06 grouped with *S. cerevisiae*, suppressor for yeast profilin 1, *syp1*, so we named SPBC4C3.06 *syp1⁺*. Figure 1 and Figure S1 illustrate the domain architecture of these proteins. The *cdc15⁺* gene is essential for viability [23], but strains with single deletions of the genes for five other F-BAR proteins were viable (Table 1). We did not attempt to isolate a *Δrga9* strain.

*Correspondence: thomas.pollard@yale.edu

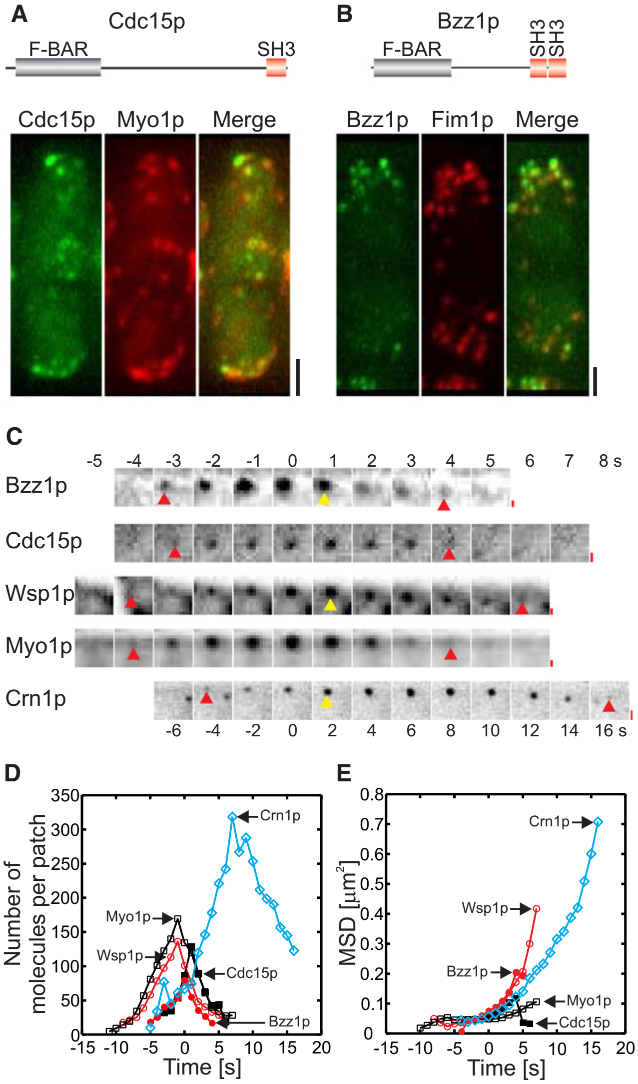

Figure 1. Quantitative Analysis of Actin Patch Dynamics

(A and B) Domain organization and localization of Cdc15p and Bzz1p in actin patches in live cells. Images are projections of three-dimensional reconstructions.

(A) Interphase cell expressing mYFP-Cdc15p (left panel, green) and mCFP-Myo1p (middle panel, red). Merged image shows Cdc15p overlaps with Myo1p in many but not all actin patches because they represent different points in time (right panel). Scale bar represents 2 μm.

(B) Interphase cell expressing Bzz1p-mEGFP (left panel, green) and an actin binding protein fimbrin (middle panel, red), Fim1p-mCherry. Merged image shows that Bzz1p overlaps with Fim1p in many but not all actin patches (right panel). Scale bar represents 2 μm.

(C) Montage of fluorescent micrographs (negative contrast images) of the time courses of Bzz1p-mEGFP, mEGFP-Cdc15p, mEGFP-Wsp1p, mEGFP-Myo1p, and Crn1p-mEGFP accumulation and loss in actin patches. Regions of 12 × 12 pixels with an actin patch are shown at 1 s intervals for all proteins except for Crn1p-mEGFP, which is shown at 2 s intervals. Red arrows show the frame where the protein appeared and the last frame before it disappeared. Yellow arrows mark the frame where the patch started to move. Scale bar represents 0.1 μm.

(D) Time courses of the accumulation and loss of five actin patch proteins. Time zero seconds marks the initiation of patch movement. The following symbols are used: Wsp1p (○, n = 20); Myo1p (□, n = 18); Cdc15p (■, n = 20); Bzz1p (●, n = 15); and Crn1p (◇, n = 30).

(E) Time course of the mean square displacement (MSD) of actin patches marked with Wsp1p (○, n = 20), Myo1p (□, n = 18), Cdc15p (■, n = 20), Bzz1p (●, n = 15), and Crn1p (◇, n = 30).

We expressed all seven F-BAR proteins fused with a monomeric fluorescent protein from their native loci under the control of their endogenous promoters. Cdc15p was tagged on the N terminus [31], whereas the monomeric fluorescent protein was fused to the C termini of the other proteins. All of the strains depending on F-BAR proteins tagged with mNFPs were viable and grew normally (Figure S1J). Syp1p is associated with early stages of endocytosis, Cdc15p and Bzz1p are associated with actin patches, and each of the other four F-BAR proteins had a unique temporal and spatial distribution in cells (Figures 1A and 1B; Figures S1B–S1I; Table 1). Cdc15p is unique among these proteins, because it participates in both endocytosis and cytokinesis [23, 32] (Figure 1A; Figure S1B). Similar to *S. cerevisiae* Bzz1p, *S. pombe* Bzz1p-mNFP concentrated in punctate structures at the tips of cells that we confirmed to be actin patches by colocalization of Bzz1p-mEGFP with the actin patch markers fimbrin or coronin tagged with mCherry (Figure 1B; data not shown).

Our study focused on actin patches, so we tested whether mEGFP-tagged Cdc15p and Bzz1p were functional by crossing these strains with mutants that exhibit synthetic interaction phenotypes when combined with mutations of the *cdc15*$^{+}$ or *bzz1*$^{+}$ genes (Table 2; see below). The mEGFP-Cdc15p fusion protein was functional because a genetic cross between *mEGFP-cdc15* and a Δ*wsp1* strain produced viable Δ*wsp1* cells expressing mEGFP-Cdc15p. mEGFP-Cdc15p localized to actin patches and contractile rings in Δ*wsp1* cells (Figure S1K). Our failure to generate *Δmyo*1 mutant cells expressing Bzz1p-mEGFP revealed that Bzz1p-mEGFP was not fully functional, but an endocytosis assay with FM4-64 showed that cells depending on Bzz1p-mEGFP took up the fluorescent dye as well as wild-type cells (Figure S1M). Bzz1p tagged on its N terminus was less functional, because mEGFP-Bzz1p expressed from the native locus failed to localize to the actin patches (Figure S1L), and crosses with Δ*myo1* cells produced only two or three viable spores.

Time Course of Cdc15p and Bzz1p Assembly in Actin Patches

Time-lapse microscopy of live cells expressing fluorescent fusion proteins established the timing of the accumulation and disappearance of Cdc15p and Bzz1p in actin patches compared with tagged Wsp1p, Myo1p, and coronin Crn1p (Figures 1C and 1D). We used the fluorescence intensity of actin patches in cells expressing single fluorescent fusion proteins to measure the numbers of molecules at 1 s time intervals [33, 34] (Figures 1C and 1D; Figures S2E–S2H and S2M). We used two criteria to align all of the measured proteins on the same timescale: the initial movement of patches was defined as time zero, and for patch components such as Myo1p and Cdc15p that did not move, we confirmed their relative positions over time by imaging strains expressing a pair of fluorescent proteins tagged with mYFP and mCFP (Figures S2A–S2D).

Bzz1p-mEGFP and mEGFP-Cdc15p appeared in, peaked, and disappeared from actin patches over ~10 s (Figure 1D; Figures S2E and S2F). The two proteins remained together in actin patches until they reached their peak concentrations and then began to separate. Myo1p peaked at ~170 (±36; one standard deviation) molecules ~2 s earlier than Cdc15p, but their numbers were equal when Cdc15p peaked at about 130 (±27) molecules (Figure 1D; Figures S2F and S2G). Both Cdc15p and Myo1p were stationary as their numbers declined (0.05 ± 0.07 μm and 0.03 ± 0.04 μm from the origin) (Figures

Table 1. *S. pombe* F-BAR Proteins

	Localization		
Gene/ Protein	Interphase	Mitosis	Deletion Mutant
cdc15/ Cdc15p	actin patches	contractile ring	nonviable
bzz1/ Bzz1p	actin patches	actin patches	viable
imp2/ Imp2p	cytoplasm	contractile ring	viable
syp1/ Syp1p	membrane/actin patches	membrane/actin patches	viable
rga7/ Rga7p	cell tips	cell tips, contractile ring and septum	viable
rga8/ Rga8p	cell tips	septum	viable
rga9/ Rga9p	cytoplasm	cytoplasm	ND[a]

[a] ND, not determined.

1C and 1E; Figures S2J and S2K). Wsp1p peaked at ~140 (±16) molecules ~1 s before Bzz1p peaked at ~75 (±15) molecules (Figures 1C and 1D; Figures S2H and S2E). Like Wsp1p (0.42 ± 0.06 µm from the origin) and verprolin Vrp1p, Bzz1p moved a short distance as it dissipated (0.25 ± 0.03 µm from the origin) (Figures 1C and 1E; Figures S2L and S2I) [35].

Genetic Interactions among Activators of Arp2/3 Complex

Wsp1p and Myo1p define two independent pathways of actin assembly at sites of endocytosis in vivo, with either pathway being sufficient for cell viability [35, 36]. To test genetic interactions with activators of Arp2/3 complex, we used a temperature-sensitive (ts) *cdc15*$^+$ mutant (*cdc15-127*) and a *bzz1*$^+$ deletion mutant with the *ura4*$^+$ gene replacing the entire *bzz1*$^+$ ORF. Cells lacking Bzz1p were shorter than wild-type cells at 25°C and grew slower than wild-type cells at higher temperatures (Table 2). We generated double-mutant strains Δ*bzz1*Δ*wsp1*, *cdc15-127* Δ*wsp1*, and *cdc15-127* Δ*myo1*, but failed to generate Δ*bzz1*Δ*myo1*, suggesting that Δ*bzz1* is synthetically lethal with Δ*myo1* (Table 2). The *cdc15-127* Δ*wsp1* strain failed to grow at temperatures greater than 25°C, suggesting that *cdc15-127* is synthetically lethal with Δ*wsp1* (Table 2). Both the *Δwsp1* and *Δmyo1* strains carried a complementing plasmid to assist in these crosses.

Table 2. Interactions between Mutations of the Genes for F-BAR Proteins Cdc15p and Bzz1p and Deletions of the Genes for the Activators of the Arp2/3 Complex Wsp1p and Myo1p

	Growth at the Indicated Temperature			
Mutant	25°C	30°C	32°C	36°C
Δbzz1	+++	+++	+++	++
cdc15-127 (ts)	+++	++	+	–
Δmyo1	++	ND[a]	ND[a]	–
Δwsp1	++	ND[a]	ND[a]	–
Δmyo1Δwsp1	–	–	–	–
Δbzz1cdc15-127(ts)	–	–	–	–
Δbzz1Δmyo1	–	–	–	–
Δbzz1Δwsp1	+++	++	++	+
cdc15-127(ts)*Δmyo1*	+++	++	++	+
cdc15-127(ts)*Δwsp1*	+++	–	–	–

The *cdc15-127* strain has a temperature-sensitive mutation that impairs contractile ring and septum formation during mitosis and rearrangement of actin patches is aberrant at restrictive temperatures. Double mutants were made by genetic crosses. Mutant strains were grown on YE5S plates with phloxin B over a range of temperatures. The symbols are as follows: growth with no or very few pink colonies (+++), growth with pink colonies (++), growth with dark pink colonies (+), and no growth (–). Dissections of asci from the cross between *Δbzz1* and *Δmyo1*, *Δwsp1*, and *Δmyo1* yielded no viable double mutants. The tetrads were either of nonparental ditype with only two viable spores or tetratype with three viable spores. Both the *Δwsp1* and *Δmyo1* strains carried a complementing plasmid to assist in these crosses.

[a] ND, not determined.

Interactions of Bzz1p and Cdc15p with Nucleation-Promoting Factors In Vivo

We isolated mutants to test the roles of Cdc15p and Bzz1p in endocytosis. The *cdc15*$^+$ gene is essential, so we replaced the endogenous promoter with a thiamine-repressible nmt1 promoter [41×] to allow thiamine to repress the level of Cdc15p 50-fold from 12 µM to 0.2 µM in wild-type cells (Figure S3A).

An endocytosis assay showed that both Bzz1p and Cdc15p are required for normal uptake of a lipophilic dye FM4-64 (Figure 2A). We used a pulse-chase design, where a cold temperature blocked endocytosis while the plasma membrane was labeled by exposing cells to 20 µM FM4-64 dye for 15 min. Raising the temperature to 25°C on the microscope stage reinitiated endocytosis, which we followed over time by fluorescence microscopy. Mutant *Δbzz1* and *41xnmt1cdc15* cells took up FM4-64 much slower than wild-type cells: by 15 min, 85% of wild-type cells but none of the *Δbzz1* cells and only 15% of *41xnmt1cdc15* cells concentrated the dye in the vacuolar membranes (Figures 2A and 2B).

Cells lacking Bzz1p or depleted of Cdc15p had serious defects in actin patch movement (Figure 2C) even though these patches contained normal amounts of Myo1p, Wsp1p, and Arp2/3 complex (Figures 2I–2K; Figures S3G–S3O). In wild-type cells, actin patches marked with coronin Crn1p-mEGFP moved persistently away from the plasma membrane (Figures 2C and 2D; Figure S3B), whereas coronin moved only ~300 nm in cells lacking Bzz1p (Figure 2C; Figure S3C), Wsp1p (Figure 2C; Figure S3F), or Myo1p (Figure 2C; Figure S3F) or depleted of Cdc15p (Figure 2C; Figure S3D). Furthermore, 38% of patches in Δ*bzz1* cells (n = 24 patches) and 19% of patches in *41xnmt1cdc15* cells (n = 32 patches) stalled or retracted back to the plasma membrane after moving a short distance (Figures 2E and 2F).

Actin patches in cells without Bzz1p or depleted of Cdc15p assembled only 20%–33% as much GFP-actin as in wild-type cells (Figure 2L; Figures S3P–S3R). GFP-tagged actin cannot replace native actin in fission yeast [33, 37], so we expressed GFP-actin from the *leu*$^+$ locus in the genome under the control of an *nmt1* promoter (medium strength *41xnmt1* promoter in *Δbzz1* cells and a strong *3xnmt1* promoter in *41xnmt1cdc15* cells). Thiamine repressed Cdc15p expression in *41xnmt1cdc15* cells, as evident from the phenotype, but the *3xnmt1* promoter allowed the cells to express about the same levels of GFP-actin in wild-type cells (3.6 μM, 11% of total actin), *Δbzz1* cells (3.2 μM, 10.3% of total actin), and *41xnmt1cdc15* cells in thiamine (4.6 μM, 15% of total actin) (Figures S3S and S3T). Control experiments verified that expression of low levels of mNFP-actin did not alter the morphology of the cells, interfere with the formation of actin cables or contractile rings, or interfere with the dynamics of other patch components tracked with CapBp (Figures S3U and S3V).

Bzz1p SH3 Domains Bind Wsp1p and Stimulate its Nucleation-Promoting Activity

We used domain deletion mutants to study the roles of the two Bzz1p SH3 domains in actin polymerization in cells. Bzz1p lacking one or both of the SH3 domains was tagged with mYFP at the C terminus and expressed at near wild-type levels from the *bzz1*$^+$ locus (Figure S4A). Bzz1p lacking a single SH3 domain accumulated in actin patches, which assembled 34% less GFP-actin (268 molecules) than wild-type cells (407 molecules) (Figure 3B). Bzz1pΔSH3ΔSH3 lacking both SH3 domains did not accumulate in actin patches (Figure 3A), and these patches assembled only 81 molecules of GFP-actin, similar to *Δbzz1* cells (Figure 3B).

Equilibrium binding assays showed that both SH3 domains of Bzz1p contribute to binding *S. pombe* Wiskott-Aldrich Syndrome protein (WASp). Purified *S. pombe* Wsp1p poly (p)-verprolin-central domain-acidic region of WASp (VCA) (residues 129–574 including the polyproline domain and VCA) bound glutathione S-transferase (GST)-Bzz1p-SH3SH3 with both SH3 domains with a much higher affinity (K_d ~0.1 μM) (Figure 3C) than GST-Bzz1p-SH3 with just the C-terminal SH3 domain (K_d ~2 μM) (Figure 3D). Neither GST nor GST-Cdc15p-SH3 bound Wsp1p poly (p)-VCA (data not shown).

Actin polymerization assays showed that dimers of Bzz1p-SH3 domains stimulate the ability of Wsp1p poly (p)-VCA to activate Arp2/3 complex (Figures 3E and 3F). Purified *S. pombe* Arp2/3 complex had little effect on the time course of spontaneous assembly of muscle actin even in the presence of 500 nM monomeric Wsp1p poly (p)-VCA with or without a monomeric construct consisting of the two Bzz1pSH3 (Figure 3E). On the other hand, the combination of Arp2/3 complex with monomeric Wsp1p poly (p)-VCA and dimeric GST-Bzz1pSH3 stimulated actin polymerization nearly as well as Arp2/3 complex with dimeric GST-Wsp1p poly (p)-VCA. The rate of actin polymerization reached a maximum with 1 μM GST-Bzz1pSH3 and 0.5 μM Wsp1p poly (p)-VCA (Figure 3F).

Myo1p Tail Is Required to Recruit Cdc15p to Patches

Experiments with deletions from the tail of Myo1p showed that the tail homology domain 2 (TH2 domain) of Myo1p is required to localize Cdc15p in actin patches, in agreement with the previous evidence from yeast two-hybrid and biochemical and immunoprecipitation assays [32]. We crossed cells expressing Cdc15p-mEGFP with *Δmyo1* cells complemented with COOH-terminal deletion mutants of Myo1p known to localize to actin patches and rescue the growth and mating defects of *Δmyo1* [36]. Cdc15p-mEGFP concentrated in actin patches with similar time courses in wild-type cells (8–12 s) and cells depending on Myo1p-H/1/2/3 (*myo1ΔA*, lacking the C-terminal A motif) or Myo1p-H/1/2 (*myo1Δ3A* lacking the C-terminal TH3 domain and A motif) (Figure S4C). However, Cdc15p-mEGFP failed to concentrate in patches of cells lacking Myo1p or depending on Myo1p without tail domains TH2, TH3, and A (*myo1Δ23A*) (Figure 3G), forming only a few spots that did not change in fluorescence intensity over time (Figure S4D).

While full-length Cdc15p-mEGFP persisted in patches for 8–12 s, small numbers of Cdc15p-mGFP lacking the single C-terminal SH3 domain (Cdc15pΔSH3-mEGFP) accumulated in patches for only ~3 s (Figure S4E) in spite of being expressed at a wild-type level from the endogenous promoter (Figure S4B). This behavior confirmed that the SH3 domain is required to concentrate Cdc15p in actin patches but not contractile rings [38]. Fic1p interacts with the SH3 domain of Cdc15p, colocalizes with Cdc15p during interphase and in mitosis, and copurifies with clathrin heavy chain, a component of the actin patch [38]. Further work will be required to understand the role of Fic1p in clathrin-mediated endocytosis and its contribution to the function of Cdc15p.

Discussion

Localization and deletion of all seven F-BAR proteins and detailed analysis of two of these proteins suggest that each F-BAR protein has a distinct function in yeast cells, even along the pathway of clathrin-mediated endocytosis [23–29, 38]. Remarkably, one F-BAR protein, Cdc15p, has distinct roles in both endocytosis and cytokinesis [32]. The functional specificity of these proteins depends on unique properties of their F-BAR domains, which have very diverse amino acid sequences beyond the conserved amino acids. For example, long stretches of amino acids unique to Cdc15p link the α helices of the F-BAR domain. Spatial and temporal variations in the lipid composition of fission yeast plasma membrane may influence the distributions of Cdc15p, Rga7p, and Rga8p to different parts of the cell during the cell cycle. Rga7p and Rga8p also include Rho GTPase activating protein domains at their C termini and are localized to the cell tips during interphase and equatorial region during cell division.

Steps in Clathrin-Mediated Endocytosis

Endocytosis in fission and the budding yeasts shares many common features, some with parallels in animal cells. Both yeasts require actin polymerization to form tubular invaginations of plasma membrane against turgor pressure [9, 39]. Fluorescence microscopy of live budding and fission yeast cells [5, 35] and electron microscopy of budding yeast [9] provided enough quantitative information [40] to formulate and test a mathematical model of actin assembly and turnover at sites of endocytosis [41]. In both yeasts, endocytosis occurs in at least three steps [1–4] (Figure 4). We use the actin patch timescale of Sirotkin et al. [40] with time zero defined as the time when actin patch components move away from the plasma membrane.

Cells initiate endocytosis more than a minute before time zero by concentrating F-BAR protein Syp1p (both yeasts) or FCHo1/2 (animals) locally in the plasma membrane [42–45]. The F-BAR domains of these proteins bind PIP_2 and demark the membrane for a new endocytic event. By time −30 s, an early module of proteins, consisting of clathrin (Clc1p and Chc1p), an Eps15 homology (EH)-domain containing protein Ede1p (in budding yeast), and adaptor proteins Pan1p and End4p (Sla2p in budding yeast), assemble on shallow (<50 nm) invaginations of the plasma membrane [40, 42, 45] with the clathrin coat occupying about 30 nm at the tip of the invagination [9]. Syp1p and Ede1p disappear near the onset of actin polymerization [42, 43], whereas clathrin remains associated with the invaginating membrane.

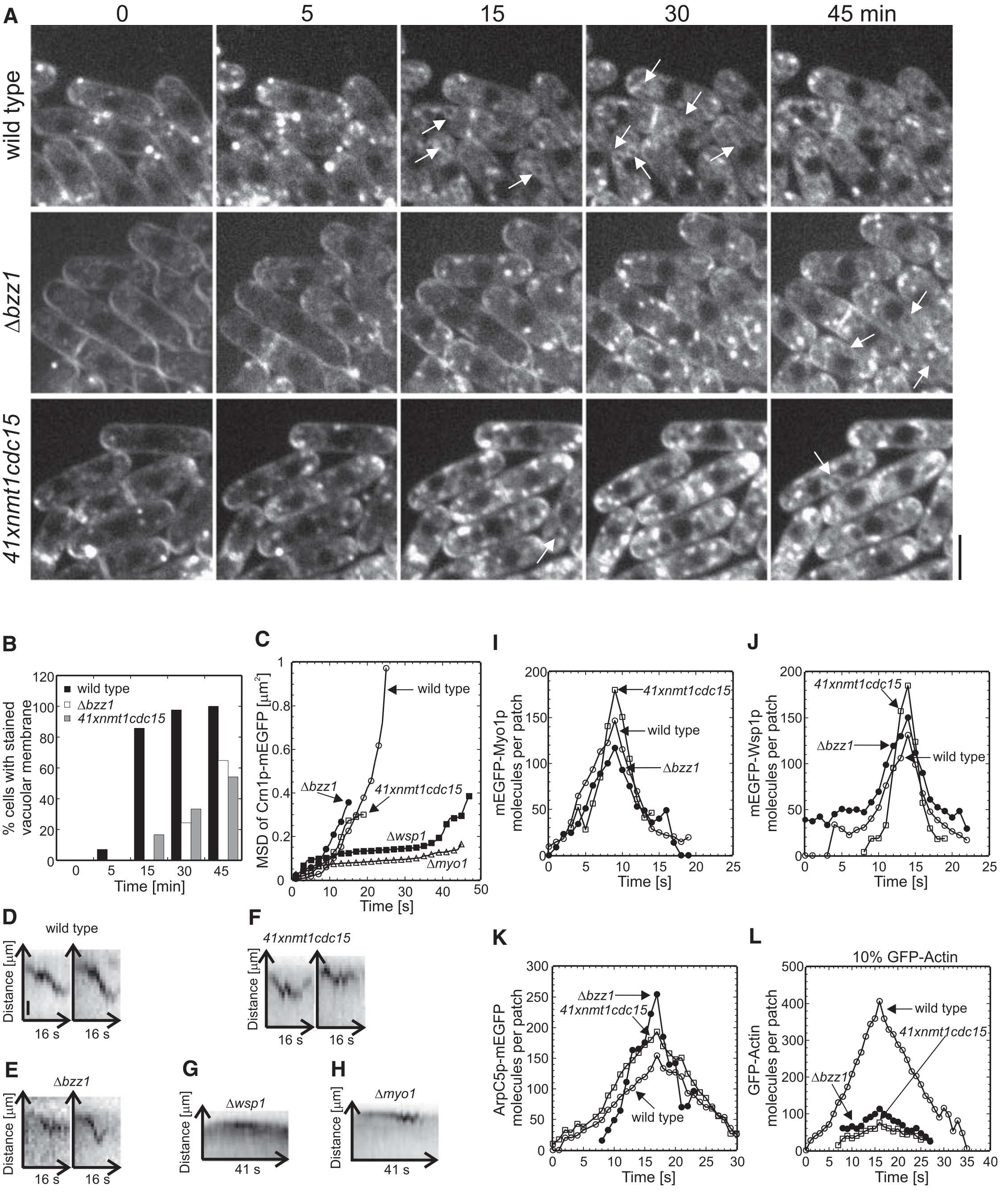

Figure 2. Effects of Bzz1p Deletion or Cdc15p Depletion on Endocytosis and Accumulation and Loss of Myo1p, Wsp1p, Arp2/3 Complex, and Actin in Actin Patches

(A) Uptake of the fluorescent dye FM4-64 by endocytosis. Wild-type, Δ*bzz1*, and *41xnmt1cdc15* cells were incubated on ice for 15 min to block endocytosis, exposed to 20 μM FM4-64 in YE5S at 4°C for 15 min, and shifted to 25°C to restart endocytosis. The images are single optical sections through the middle of the cells at different time points. White arrows mark fluorescent vacuolar membranes. The rows show wild-type cells (top), *Δbzz1* cells (middle), and *41xnmt1cdc15* cells depleted of Cdc15p (bottom). Scale bar represents 5 μm.

(B) Quantitative analysis of endocytosis by scoring cells in time-lapse movies that concentrated FM4-64 dye in the vacuolar membranes: wild-type cells (black bars; n = 42), *Δbzz1* cells (white bars; n = 39), and *41xnmt1cdc15* cells (gray bars; n = 24).

(C–H) Movements of actin patches tagged with coronin Crn1p-mEGFP in wild-type and mutant cells.

(C) MSD of the diffraction-limited spot of Crn1p-mEGFP fluorescence over time. The following symbols are used: wild-type cells (○, n = 10), *Δbzz1* cells lacking Bzz1p (●, n = 12), *41xnmt1cdc15* cells depleted of Cdc15p (□, n = 13), *Δwsp1* cells lacking Wsp1p (■, n = 12), and *Δmyo1* cells lacking Myo1p (Δ, n = 11).

(D–H) Kymographs of individual Crn1p-mEGFP patches from five confocal sections imaged at 1 s intervals. A 24 × 14 pixel box was sum projected into a 24 × 1 pixel vertical lane and 16 lanes (D–F) or 41 lanes (G and H) were combined horizontally to generate negative contrast kymographs. Panels are shown as follows: wild-type cells (D), *Δbzz1* cells (E), *41xnmt1cdc15* cells (F), *Δwsp1* cells (G), and *Δmyo1* cells (H). Vertical black scale bar represents 100 nm.

(I–L) Time courses of the accumulation and loss of actin patch proteins at 25°C in wild-type cells (○), *Δbzz1* strains lacking Bzz1p (●), and *41xnmt1cdc15* cells depleted of Cdc15p (□).

During the second step beginning at time −11 s, nucleation-promoting factors Wsp1p and Myo1p start to accumulate followed by F-BAR proteins Bzz1p and Cdc15p (Figure 1D). These four proteins promote assembly of actin filaments by Arp2/3 complex starting at time −6 s. We show that fission yeast require an F-BAR protein in addition to Arp2/3 complex and either Wsp1p or Myo1p [35] for actin polymerization, patch movement, and uptake of FM4-64. The movement of patch components in budding yeast corresponds to invagination of a narrow tubule of plasma membrane into the cytoplasm [9]. Given the similarity of the process in the two fungi, we assume that this applies to fission yeast. The movement of actin patches in budding yeast depends on both the Arp2/3 complex activation and motor activity of type I myosins [18].

The numbers and locations of proteins associated with actin patches provide the basis to predict the structures formed by the F-BAR proteins. F-BAR domains bind to lipid bilayers and induce membrane tubulation or assemble helical structures around tubular membranes [46]. A membrane tubule 57 nm in diameter can accommodate eight F-BAR dimers around its circumference, so the peak number of 80 Bzz1p molecules would wrap around the tubular invagination five times and occupy as little as 20 nm along the length of the tubule. Electron micrographs suggested that the F-BAR domains of Cdc15p might be as long as 30 nm [47], so the peak number of 130 molecules might wrap ~8 times around the membrane invagination. These two zones of F-BAR proteins are not resolved by confocal fluorescence microscopy early in the process, but starting at time zero, the center of the diffraction-limited spot of Bzz1p starts to move up to 250 nm from the cluster of Cdc15p, which is left behind in its original location near the cell surface. Therefore we expect that a 30 nm cuff of Cdc15p forms and remains close to the base of the tubule, whereas the 20 nm cuff of Bzz1p moves with the clathrin-coated tip of the invaginating tubule (Figure 4). Assuming that these F-BAR domains decorate the membrane in a closely packed helical array, our molecule counts show that the F-BAR proteins concentrate a high density of SH3 domains on these membrane invaginations: ~45,000 SH3 domains/μm^2 at the tip (two SH3 domains/Bzz1p molecule) and ~16,500 SH3 domains/μm^2 near the neck of the tubular invagination (one SH3 domain from Cdc15p). The high density of Bzz1p SH3 domains is expected to activate Wsp1p, because dimers of WASp-VCA are much more effective in stimulating Arp2/3 complex than monomers [48, 49].

One surprise is that recruitment of the F-BAR proteins follows in time and depends on the nucleation-promoting factors, because the F-BAR domains presumably associate with the membrane tubule, and it is easier to envisage a layered structure forming outward from the membrane surface with the F-BAR proteins acting as adapters between the membrane and their partners, the nucleation-promoting factors. Further work is required to clarify this conundrum.

In addition to recruiting F-BAR proteins to sites of endocytosis, NPFs may activate the F-BAR proteins to tubulate membranes. Structural studies showed that the SH3 domain of the full-length F-BAR protein syndapin inhibits the potent membrane deforming activity and that ligand binding to the SH3 domain unclamps the protein leading to membrane deformation [50, 51]. Thus SH3 domains of F-BAR proteins may serve both inhibitory and targeting roles [52].

Role of F-BAR Proteins in *S. pombe* Endocytic Vesicle Scission

The endocytic vesicle separates from the plasma membrane during the third step. In animal cells, scission of the vesicle depends on dynamin and occurs just before dissociation of the clathrin coat [53]. Actin patch movements, vesicle scission, and endocytosis in fungi are compromised in the absence of Wsp1p, Myo1p, Cdc15p, or Bzz1p, so this step depends on the contributions of each of these proteins to actin polymerization [39]. The time of scission has not been documented in fungi, but we suggest that it occurs at about time +6 s when clathrin and coronin move beyond Wsp1p and Vrp1p, which stop moving about 300–400 nm from the cell surface. In cells lacking either Bzz1p or Cdc15p, patches marked with coronin either move only short distances from the cell surface or retract back to the cell surface, so we suggest that vesicles loaded with the cargo fail to pinch off at this step and remain associated with the plasma membrane as a consequence of this lack of movement. Clathrin disassociates when it moves about 500 nm from the plasma membrane [5, 40], whereas coronin moves up to 800 nm into the cytoplasm.

Our observations provide clues regarding the roles of F-BAR proteins in actin polymerization associated with endocytosis and suggest a possible mechanism of vesicle scission (Figure 4). Because Bzz1p and Wsp1p separate from Cdc15p and Myo1p after time zero, actin polymerization driven by these nucleation-promoting factors should concentrate actin filament formation in two zones along the invaginated membrane tubule. A ring of Cdc15p and Myo1p might stimulate one zone of actin assembly near the cell surface. A ring of activated Wsp1p would concentrate actin filament formation in a second zone near the tip of the invaginated membrane tubule. We suggest that the movement of Bzz1p and Wsp1p with most other patch proteins corresponds to the elongation of tubular invagination of the plasma membrane.

We propose that the two rings of F-BAR proteins and their partner nucleation-promoting factors produce two opposing zones of actin polymerization that push against each other to elongate the tubular invagination of the plasma membrane, which breaks to release the coated vesicle (Figure 4). The high density of branched filaments arising in these two zones should preclude their interpenetration, allowing polymerization to produce force to stretch the membrane and contribute to scission of the vesicle without requiring precise orientation of the filaments relative to the membrane.

This new idea complements previous proposals to explain the vesicle scission. The "mechanochemical" model

(I) mEGFP-Myo1p was expressed from the native locus and the numbers of molecules per patch were tracked over time in wild-type cells (n = 21 patches), *41xnmt1cdc15* cells (n = 15), and *Δbzz1* cells (n = 12).

(J) mEGFP-Wsp1p was expressed from the native locus and the numbers of molecules per patch were tracked over time in wild-type cells (n = 12 patches), *41xnmt1cdc15* cells (n = 23), and *Δbzz1* cells (n = 18).

(K) The Arp2/3 complex subunit ArpC5p-mEGFP was expressed from the native locus and the numbers of molecules per patch were tracked over time in wild-type cells (n = 12), *41xnmt1cdc15* cells (n = 7), and *Δbzz1* cells (n = 8).

(L) GFP-actin was expressed from the *leu*$^+$ locus in the presence of wild-type levels of native actin from a 41xnmt1 promoter in wild-type cells (○), Δ*bzz1* cells lacking Bzz1p (●), and from a 3xnmt1 promoter in *41xnmt1cdc15* cells (□). The numbers of molecules per patch were tracked over time.

[54] focuses on the contributions of the membrane lipids and the actin cytoskeleton. BAR domain proteins are proposed to bind and protect PIP$_2$ from hydrolysis by phosphatidylinositol phosphatases in the tubular invagination of the plasma membrane. Hydrolysis of PIP$_2$ elsewhere along the tubular invagination generates PIP. The mobility of PIP and immobility of PIP$_2$ bound to BAR domain proteins produce a lipid phase separation that changes the membrane tension along the boundary between the two phases [54, 55]. The change in membrane tension coupled to the pulling and pushing forces of actin cytoskeleton and myosin I at the plasma membrane generate vesicle scission. An alternative model [56] based on in vitro reconstitution experiments proposes that BAR domain proteins mediate assembly of actin filaments at an angle to the invaginating membrane providing a pushing force that squeezes the membrane tubule and facilitates fission of the vesicle. The localization of overexpressed Las17 (budding yeast WASp) on the invaginating membrane [57] is consistent with this hypothesis. Much more information about the organization of the molecules in actin patches is required to evaluate all of these hypotheses.

The overall pathway of endocytic patch assembly is similar in budding and fission yeast, but subtle differences include the total lifetime of the patches and the numbers of some patch proteins. Actin patches in *S. cerevisiae* depend on Bzz1p to activate the Wsp1p homolog Las17p [58] but appear to lack a second F-BAR protein. However, type I myosin Myo5p localizes with actin filaments to a different part of the plasma membrane invaginations than Bzz1p and Las17p [9], so two zones of actin polymerization may also contribute to endocytosis in budding yeast.

Experimental Procedures

Strain Construction, Growth Conditions, and Cellular Methods

Table S1 lists the *S. pombe* strains used in this study. We generated all strains by PCR-based gene targeting [59, 60] and standard genetic methods [60]. FM4-64 assay for endocytosis was performed as described previously. We stained cells with BODIPY 488-phalloidin (Invitrogen) [61].

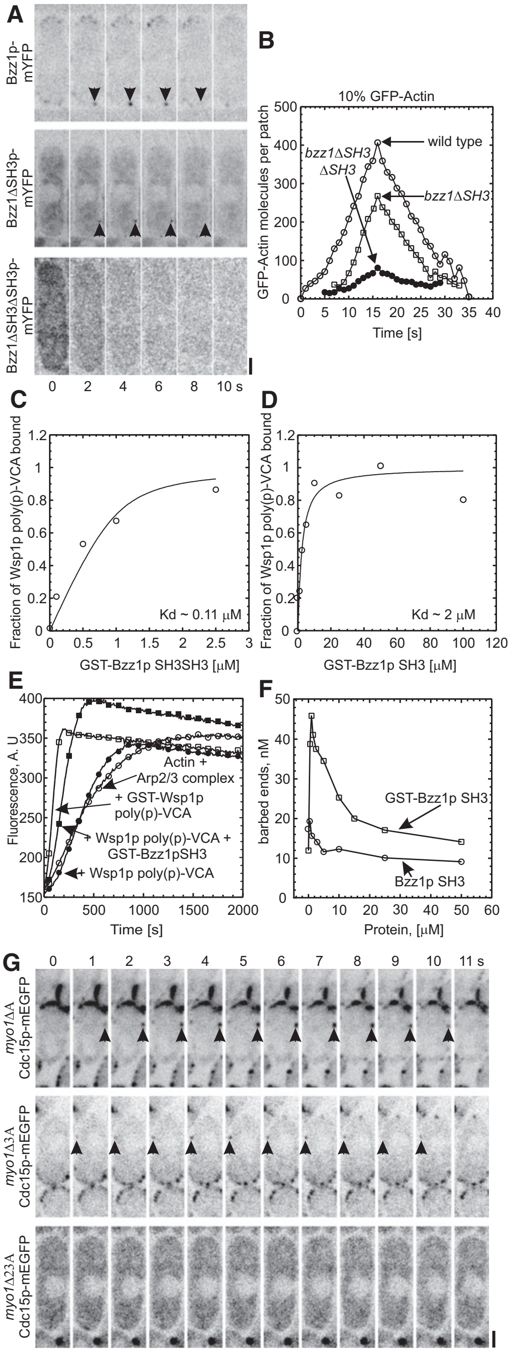

Figure 3. Interactions between F-BAR Proteins and Nucleation-Promoting Factors in Actin Polymerization in Actin Patches

(A) Influence of Bzz1p SH3 domains on accumulation of the protein in actin patches. Time series of negative contrast fluorescence micrographs of single confocal sections at 2 s intervals: Bzz1p-mYFP (upper row); Bzz1pΔSH3-mYFP (middle row); and Bzz1pΔSH3ΔSH3-mYFP cells (lower row).

(B) Influence of Bzz1p SH3 domains on accumulation of GFP-actin in actin patches. GFP-actin was expressed from a 41xnmt1 promoter from the *leu$^+$* locus in wild-type cells (○), *bzz1ΔSH3* cells lacking the C-terminal SH3 domain (□), or *bzz1ΔSH3ΔSH3* cells lacking both the SH3 domains (●). The numbers of molecules per patch were tracked over time.

(C and D) Equilibrium binding of Bzz1p SH3 domains to Wsp1p-poly (p)-VCA. Soluble 1 μM Wsp1p poly (p)-VCA was incubated with a range of concentrations of glutathione beads with bound GST-Bzz1pSH3SH3 (residues 521–642) (C) or GST-Bzz1pSH3 (residues 586–642) (D) at room temperature in 25 mM Tris-HCl pH 7.4, 75 mM NaCl, 1 mM EDTA, 1 mM dithiothreitol (DTT). Beads were pelleted at 16,000 × g and the bound fraction was calculated from concentration of Wsp1p poly (p)-VCA in the supernatant quantified by sodium dodecyl sulfate polyacrylamide gel electrophoresis (SDS-PAGE), staining with Coomassie blue and densitometry. Equilibrium dissociation constants (K$_d$) were determined by fitting data to binding isotherms (solid lines).

(E and F) Effects of Bzz1p SH3 domains on the nucleation-promoting activity of Wsp1p. Time course of the polymerization of actin measured by the fluorescence of pyrenyl-actin. All samples contained 4 μM actin (10% pyrenyl-actin) and 50 nM *S. pombe* Arp2/3 complex in KMEI buffer.

(E) Dependence on nucleation-promoting factors: no additions (○), 500 nM Wsp1p-poly (p)-VCA (●), 500 nM GST-Wsp1p-poly (p)-VCA (□), 500 nM Wsp1p-poly (p)-VCA (■), and 1 μM GST-Bzz1pSH3.

(F) Dependence of the numbers of actin filament barbed ends created by 4 μM actin (10% pyrenyl-actin), 50 nM Arp2/3 complex, and 500 nM Wsp1p-poly (p)-VCA on the concentration of GST-Bzz1pSH3 (□) or Bzz1pSH3 (o).

(G) Dependence of Cdc15p-mEGFP targeting to actin patches on tail domains of Myo1p. Time series of negative contrast fluorescence micrographs at 1 s intervals of single confocal planes through cells depending on Cdc15p-mEGFP and with Myo1p lacking domains: *myo1ΔA* lacking the acidic motif (upper panel); *myo1Δ3A* lacking tail homology domain 3 and acidic motif (middle panel); and *myo1Δ23A* lacking tail homology domains 2 and 3 and the acidic motif (lower panel). Black arrowheads indicate Cdc15p-mEGFP in patches. Scale bar represents 1 μm.

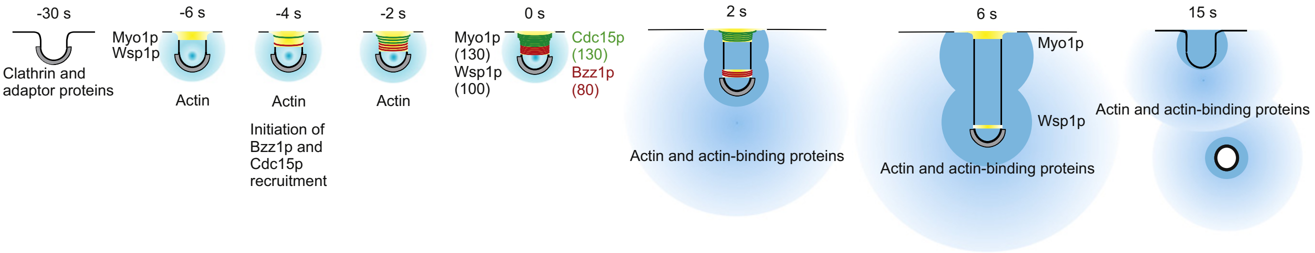

Figure 4. Hypothesis for the Contributions of F-BAR Proteins Cdc15p and Bzz1p to Endocytosis

Eight time points in the life of an actin patch with time zero defined as the onset of movement of patch proteins away from the plasma membrane. The plasma membrane is a black line, clathrin is gray, nucleation-promoting factors Wsp1p and Myo1p are yellow, Cdc15p is green, Bzz1p is red, actin filaments are blue, and numbers of molecules are in parentheses. Clathrin is recruited 2 min prior to invagination. Nucleation-promoting factors are recruited beginning at −10 s and peak prior to patch movement at −2 s (Figures 1C–1E). F-BAR proteins Cdc15p and Bzz1p begin to accumulate at −5 s and peak at the onset of patch movement (Figures 1C–1E). Recruitment of Cdc15p requires Myo1p (Figure 3G), and both the proteins remain near the cell surface. Bzz1p binds and activates Wsp1p to stimulate the assembly of branched actin filaments by Arp2/3 complex (Figures 3C–3F). We assume that movement of Bzz1p, Wsp1p, and many other patch proteins is associated with elongation of the plasma membrane tubule. We propose that expansion of branched filaments from two distinct zones of NPFs pushes the tip of the invaginating tubule away from the cell surface (2–6 s) (Figure 1E) contributing to scission of the coated vesicle. Both F-BAR proteins dissociate from the invaginating tubule as the vesicle moves into the cytoplasm (Figure 1D).

Microscopy and Data Analysis

Fluorescence images of live cells were acquired with an Olympus IX-71 microscope with a 100×/NA 1.4 Plan Apo lens (Olympus) and an UltraView RS (PerkinElmer) or CSU-X1 (Andor Technology) confocal spinning disk confocal system equipped with an ORCA-ER CCD camera (Hamamatsu Corporation) or iXON-EMCCD camera (Andor Technology). Cells were imaged on 25% gelatin in EMM5S at 25°C. Patches were tracked using custom ImageJ plugins on images corrected for uneven illumination and camera noise. Fluorescence intensities of patches and the mean square displacements of patches over time were calculated from the sum-projected two-dimensional images. See Supplemental Experimental Procedures for detailed information on image acquisition and data analysis.

Bacterial Expression Constructs and Protein Purification

S. pombe proteins Arp2/3 complex, Myo1pTH2-SH3-CA, Wsp1p poly (p)-VCA (proline-rich domain, verprolin homology motif, connecting motif and acidic motif, nucleotides 385–1725), Bzz1pSH3SH3 (nucleotides 1561–1929); Bzz1pSH3 (nucleotides 1757–1929), and Cdc15pSH3 (nucleotides 2607–2784) were used in our biochemical experiments. For details on the cloning and purification of these proteins, see Supplemental Experimental Procedures.

Quantitative Pull-Down Assays

Equilibrium dissociation constants (K_d) were measured by quantitative pull-down assays [62]. We used KaleidaGraph (Synergy Software) to fit a binding isotherm to the dependence of the fraction of ligand bound $[LR]/[L_{tot}]$ to $[L_{tot}]$ using the equation $[LR]/[L_{tot}] = (([R] + [L_{tot}] + K_d) - (([R] + [L_{tot}] + K_d)^2 - 4 \times [R] \times [L])^{0.5})/2 \times [L_{tot}]$.

Actin Polymerization Assays

The time course of actin polymerization was measured by fluorescence of pyrene-labeled actin in 10 mM imidazole, 1 mM $MgCl_2$, 1 mM EGTA, 50 mM KCl [63]. Polymerization rates were measured from the time courses of actin polymerization when half of actin was polymerized. We measured the concentration of ends from the rate of elongation by using the following relationship: $R = k_+(A)(ends) - k_-(ends)$, where R is the rate of elongation, k_+ is the association rate constant (11.6 $\mu M^{-1} s^{-1}$), k_- is the dissociation rate constant (1.4 s^{-1}), A is the concentration of actin monomer, and *ends* is the concentration of growing filament ends [64, 65].

Supplemental Information

Supplemental Information includes four figures, one table, Supplemental Experimental Procedures, and Supplemental Results and can be found with this article online at doi:10.1016/j.cub.2011.07.046.

Acknowledgments

We are grateful to Kathleen L. Gould (Vanderbilt University School of Medicine) and Vladimir Sirotkin (Upstate Medical University) for yeast strains. We thank Julien Berro, Vladimir Sirotkin, and Chad McCormick for help with image analysis and valuable advice. We thank Irene Reynolds Tebbs and Tara Reisbig for help with patch tracking. This work was supported by National Institutes of Health research grants GM-026132 and GM-026338.

Received: May 10, 2010
Revised: June 30, 2011
Accepted: July 27, 2011

References

1. Kaksonen, M., Toret, C.P., and Drubin, D.G. (2006). Harnessing actin dynamics for clathrin-mediated endocytosis. Nat. Rev. Mol. Cell Biol. *7*, 404–414.
2. Conner, S.D., and Schmid, S.L. (2003). Regulated portals of entry into the cell. Nature *422*, 37–44.
3. Doherty, G.J., and McMahon, H.T. (2009). Mechanisms of endocytosis. Annu. Rev. Biochem. *78*, 857–902.
4. Galletta, B.J., and Cooper, J.A. (2009). Actin and endocytosis: Mechanisms and phylogeny. Curr. Opin. Cell Biol. *21*, 20–27.
5. Kaksonen, M., Toret, C.P., and Drubin, D.G. (2005). A modular design for the clathrin- and actin-mediated endocytosis machinery. Cell *123*, 305–320.
6. Itoh, T., Erdmann, K.S., Roux, A., Habermann, B., Werner, H., and De Camilli, P. (2005). Dynamin and the actin cytoskeleton cooperatively regulate plasma membrane invagination by BAR and F-BAR proteins. Dev. Cell *9*, 791–804.
7. Yu, X., and Cai, M. (2004). The yeast dynamin-related GTPase Vps1p functions in the organization of the actin cytoskeleton via interaction with Sla1p. J. Cell Sci. *117*, 3839–3853.
8. Nannapaneni, S., Wang, D., Jain, S., Schroeder, B., Highfill, C., Reustle, L., Pittsley, D., Maysent, A., Moulder, S., McDowell, R., and Kim, K. (2010). The yeast dynamin-like protein Vps1: Vps1 mutations perturb the internalization and the motility of endocytic vesicles and endosomes via disorganization of the actin cytoskeleton. Eur. J. Cell Biol. *89*, 499–508.
9. Idrissi, F.Z., Grötsch, H., Fernández-Golbano, I.M., Presciatto-Baschong, C., Riezman, H., and Geli, M.I. (2008). Distinct acto/myosin-I structures associate with endocytic profiles at the plasma membrane. J. Cell Biol. *180*, 1219–1232.
10. Röthlisberger, S., Jourdain, I., Johnson, C., Takegawa, K., and Hyams, J.S. (2009). The dynamin-related protein Vps1 regulates vacuole fission, fusion and tubulation in the fission yeast, Schizosaccharomyces pombe. Fungal Genet. Biol. *46*, 927–935.

11. Pelkmans, L., Püntener, D., and Helenius, A. (2002). Local actin polymerization and dynamin recruitment in SV40-induced internalization of caveolae. Science *296*, 535–539.
12. Yarar, D., Waterman-Storer, C.M., and Schmid, S.L. (2005). A dynamic actin cytoskeleton functions at multiple stages of clathrin-mediated endocytosis. Mol. Biol. Cell *16*, 964–975.
13. Merrifield, C.J., Perrais, D., and Zenisek, D. (2005). Coupling between clathrin-coated-pit invagination, cortactin recruitment, and membrane scission observed in live cells. Cell *121*, 593–606.
14. Merrifield, C.J., Feldman, M.E., Wan, L., and Almers, W. (2002). Imaging actin and dynamin recruitment during invagination of single clathrin-coated pits. Nat. Cell Biol. *4*, 691–698.
15. Swanson, J.A., and Watts, C. (1995). Macropinocytosis. Trends Cell Biol. *5*, 424–428.
16. Saffarian, S., Cocucci, E., and Kirchhausen, T. (2009). Distinct dynamics of endocytic clathrin-coated pits and coated plaques. PLoS Biol. *7*, e1000191.
17. Kaksonen, M., Sun, Y., and Drubin, D.G. (2003). A pathway for association of receptors, adaptors, and actin during endocytic internalization. Cell *115*, 475–487.
18. Sun, Y., Martin, A.C., and Drubin, D.G. (2006). Endocytic internalization in budding yeast requires coordinated actin nucleation and myosin motor activity. Dev. Cell *11*, 33–46.
19. Newpher, T.M., Smith, R.P., Lemmon, V., and Lemmon, S.K. (2005). In vivo dynamics of clathrin and its adaptor-dependent recruitment to the actin-based endocytic machinery in yeast. Dev. Cell *9*, 87–98.
20. Engqvist-Goldstein, A.E., Kessels, M.M., Chopra, V.S., Hayden, M.R., and Drubin, D.G. (1999). An actin-binding protein of the Sla2/Huntingtin interacting protein 1 family is a novel component of clathrin-coated pits and vesicles. J. Cell Biol. *147*, 1503–1518.
21. Tsujita, K., Suetsugu, S., Sasaki, N., Furutani, M., Oikawa, T., and Takenawa, T. (2006). Coordination between the actin cytoskeleton and membrane deformation by a novel membrane tubulation domain of PCH proteins is involved in endocytosis. J. Cell Biol. *172*, 269–279.
22. Yarar, D., Waterman-Storer, C.M., and Schmid, S.L. (2007). SNX9 couples actin assembly to phosphoinositide signals and is required for membrane remodeling during endocytosis. Dev. Cell *13*, 43–56.
23. Fankhauser, C., Reymond, A., Cerutti, L., Utzig, S., Hofmann, K., and Simanis, V. (1995). The S. pombe cdc15 gene is a key element in the reorganization of F-actin at mitosis. Cell *82*, 435–444.
24. Low, C.P., Shui, G., Liew, L.P., Buttner, S., Madeo, F., Dawes, I.W., Wenk, M.R., and Yang, H. (2008). Caspase-dependent and -independent lipotoxic cell-death pathways in fission yeast. J. Cell Sci. *121*, 2671–2684.
25. Demeter, J., and Sazer, S. (1998). imp2, a new component of the actin ring in the fission yeast Schizosaccharomyces pombe. J. Cell Biol. *143*, 415–427.
26. Nakano, K., Mutoh, T., and Mabuchi, I. (2001). Characterization of GTPase-activating proteins for the function of the Rho-family small GTPases in the fission yeast Schizosaccharomyces pombe. Genes Cells *6*, 1031–1042.
27. Soto, T., Villar-Tajadura, M.A., Madrid, M., Vicente, J., Gacto, M., Pérez, P., and Cansado, J. (2010). Rga4 modulates the activity of the fission yeast cell integrity MAPK pathway by acting as a Rho2 GTPase-activating protein. J. Biol. Chem. *285*, 11516–11525.
28. Villar-Tajadura, M.A., Coll, P.M., Madrid, M., Cansado, J., Santos, B., and Pérez, P. (2008). Rga2 is a Rho2 GAP that regulates morphogenesis and cell integrity in S. pombe. Mol. Microbiol. *70*, 867–881.
29. Yang, P., Qyang, Y., Bartholomeusz, G., Zhou, X., and Marcus, S. (2003). The novel Rho GTPase-activating protein family protein, Rga8, provides a potential link between Cdc42/p21-activated kinase and Rho signaling pathways in the fission yeast, Schizosaccharomyces pombe. J. Biol. Chem. *278*, 48821–48830.
30. Soulard, A., Lechler, T., Spiridonov, V., Shevchenko, A., Shevchenko, A., Li, R., and Winsor, B. (2002). Saccharomyces cerevisiae Bzz1p is implicated with type I myosins in actin patch polarization and is able to recruit actin-polymerizing machinery in vitro. Mol. Cell. Biol. *22*, 7889–7906.
31. Wu, J.Q., Kuhn, J.R., Kovar, D.R., and Pollard, T.D. (2003). Spatial and temporal pathway for assembly and constriction of the contractile ring in fission yeast cytokinesis. Dev. Cell *5*, 723–734.
32. Carnahan, R.H., and Gould, K.L. (2003). The PCH family protein, Cdc15p, recruits two F-actin nucleation pathways to coordinate cytokinetic actin ring formation in Schizosaccharomyces pombe. J. Cell Biol. *162*, 851–862.
33. Wu, J.Q., and Pollard, T.D. (2005). Counting cytokinesis proteins globally and locally in fission yeast. Science *310*, 310–314.
34. Wu, J.Q., McCormick, C.D., and Pollard, T.D. (2008). Chapter 9: Counting proteins in living cells by quantitative fluorescence microscopy with internal standards. Methods Cell Biol. *89*, 253–273.
35. Sirotkin, V., Beltzner, C.C., Marchand, J.B., and Pollard, T.D. (2005). Interactions of WASp, myosin-I, and verprolin with Arp2/3 complex during actin patch assembly in fission yeast. J. Cell Biol. *170*, 637–648.
36. Lee, W.L., Bezanilla, M., and Pollard, T.D. (2000). Fission yeast myosin-I, Myo1p, stimulates actin assembly by Arp2/3 complex and shares functions with WASp. J. Cell Biol. *151*, 789–800.
37. Wu, J.Q., Sirotkin, V., Kovar, D.R., Lord, M., Beltzner, C.C., Kuhn, J.R., and Pollard, T.D. (2006). Assembly of the cytokinetic contractile ring from a broad band of nodes in fission yeast. J. Cell Biol. *174*, 391–402.
38. Roberts-Galbraith, R.H., Chen, J.S., Wang, J., and Gould, K.L. (2009). The SH3 domains of two PCH family members cooperate in assembly of the Schizosaccharomyces pombe contractile ring. J. Cell Biol. *184*, 113–127.
39. Aghamohammadzadeh, S., and Ayscough, K.R. (2009). Differential requirements for actin during yeast and mammalian endocytosis. Nat. Cell Biol. *11*, 1039–1042.
40. Sirotkin, V., Berro, J., Macmillan, K., Zhao, L., and Pollard, T.D. (2010). Quantitative analysis of the mechanism of endocytic actin patch assembly and disassembly in fission yeast. Mol. Biol. Cell *21*, 2894–2904.
41. Berro, J., Sirotkin, V., and Pollard, T.D. (2010). Mathematical modeling of endocytic actin patch kinetics in fission yeast: Disassembly requires release of actin filament fragments. Mol. Biol. Cell *21*, 2905–2915.
42. Stimpson, H.E., Toret, C.P., Cheng, A.T., Pauly, B.S., and Drubin, D.G. (2009). Early-arriving Syp1p and Ede1p function in endocytic site placement and formation in budding yeast. Mol. Biol. Cell *20*, 4640–4651.
43. Boettner, D.R., D'Agostino, J.L., Torres, O.T., Daugherty-Clarke, K., Uygur, A., Reider, A., Wendland, B., Lemmon, S.K., and Goode, B.L. (2009). The F-BAR protein Syp1 negatively regulates WASp-Arp2/3 complex activity during endocytic patch formation. Curr. Biol. *19*, 1979–1987.
44. Reider, A., Barker, S.L., Mishra, S.K., Im, Y.J., Maldonado-Báez, L., Hurley, J.H., Traub, L.M., and Wendland, B. (2009). Syp1 is a conserved endocytic adaptor that contains domains involved in cargo selection and membrane tubulation. EMBO J. *28*, 3103–3116.
45. Henne, W.M., Boucrot, E., Meinecke, M., Evergren, E., Vallis, Y., Mittal, R., and McMahon, H.T. (2010). FCHo proteins are nucleators of clathrin-mediated endocytosis. Science *328*, 1281–1284.
46. Frost, A., Perera, R., Roux, A., Spasov, K., Destaing, O., Egelman, E.H., De Camilli, P., and Unger, V.M. (2008). Structural basis of membrane invagination by F-BAR domains. Cell *132*, 807–817.
47. Roberts-Galbraith, R.H., Ohi, M.D., Ballif, B.A., Chen, J.S., McLeod, I., McDonald, W.H., Gygi, S.P., Yates, J.R., 3rd, and Gould, K.L. (2010). Dephosphorylation of F-BAR protein Cdc15 modulates its conformation and stimulates its scaffolding activity at the cell division site. Mol. Cell *39*, 86–99.
48. Higgs, H.N., Blanchoin, L., and Pollard, T.D. (1999). Influence of the C terminus of Wiskott-Aldrich syndrome protein (WASp) and the Arp2/3 complex on actin polymerization. Biochemistry *38*, 15212–15222.
49. Padrick, S.B., Cheng, H.C., Ismail, A.M., Panchal, S.C., Doolittle, L.K., Kim, S., Skehan, B.M., Umetani, J., Brautigam, C.A., Leong, J.M., and Rosen, M.K. (2008). Hierarchical regulation of WASP/WAVE proteins. Mol. Cell *32*, 426–438.
50. Rao, Y., Ma, Q., Vahedi-Faridi, A., Sundborger, A., Pechstein, A., Puchkov, D., Luo, L., Shupliakov, O., Saenger, W., and Haucke, V. (2010). Molecular basis for SH3 domain regulation of F-BAR-mediated membrane deformation. Proc. Natl. Acad. Sci. USA *107*, 8213–8218.
51. Wang, Q., Navarro, M.V., Peng, G., Molinelli, E., Goh, S.L., Judson, B.L., Rajashankar, K.R., and Sondermann, H. (2009). Molecular mechanism of membrane constriction and tubulation mediated by the F-BAR protein Pacsin/Syndapin. Proc. Natl. Acad. Sci. USA *106*, 12700–12705.
52. Kumar, V., Fricke, R., Bhar, D., Reddy-Alla, S., Krishnan, K.S., Bogdan, S., and Ramaswami, M. (2009). Syndapin promotes formation of a postsynaptic membrane system in Drosophila. Mol. Biol. Cell *20*, 2254–2264.
53. Taylor, M.J., Perrais, D., and Merrifield, C.J. (2011). A high precision survey of the molecular dynamics of mammalian clathrin-mediated endocytosis. PLoS Biol. *9*, e1000604.

54. Liu, J., Sun, Y., Drubin, D.G., and Oster, G.F. (2009). The mechanochemistry of endocytosis. PLoS Biol. *7*, e1000204.
55. Liu, J., Kaksonen, M., Drubin, D.G., and Oster, G. (2006). Endocytic vesicle scission by lipid phase boundary forces. Proc. Natl. Acad. Sci. USA *103*, 10277–10282.
56. Suetsugu, S. (2009). The direction of actin polymerization for vesicle fission suggested from membranes tubulated by the EFC/F-BAR domain protein FBP17. FEBS Lett. *583*, 3401–3404.
57. Galletta, B.J., Chuang, D.Y., and Cooper, J.A. (2008). Distinct roles for Arp2/3 regulators in actin assembly and endocytosis. PLoS Biol. *6*, e1.
58. Soulard, A., Friant, S., Fitterer, C., Orange, C., Kaneva, G., Mirey, G., and Winsor, B. (2005). The WASP/Las17p-interacting protein Bzz1p functions with Myo5p in an early stage of endocytosis. Protoplasma *226*, 89–101.
59. Bähler, J., Wu, J.Q., Longtine, M.S., Shah, N.G., McKenzie, A., 3rd, Steever, A.B., Wach, A., Philippsen, P., and Pringle, J.R. (1998). Heterologous modules for efficient and versatile PCR-based gene targeting in Schizosaccharomyces pombe. Yeast *14*, 943–951.
60. Moreno, S., Klar, A., and Nurse, P. (1991). Molecular genetic analysis of fission yeast Schizosaccharomyces pombe. Methods Enzymol. *194*, 795–823.
61. Arai, R., Nakano, K., and Mabuchi, I. (1998). Subcellular localization and possible function of actin, tropomyosin and actin-related protein 3 (Arp3) in the fission yeast Schizosaccharomyces pombe. Eur. J. Cell Biol. *76*, 288–295.
62. Lee, W.L., Ostap, E.M., Zot, H.G., and Pollard, T.D. (1999). Organization and ligand binding properties of the tail of Acanthamoeba myosin-IA. Identification of an actin-binding site in the basic (tail homology-1) domain. J. Biol. Chem. *274*, 35159–35171.
63. Cooper, J.A., Walker, S.B., and Pollard, T.D. (1983). Pyrene actin: Documentation of the validity of a sensitive assay for actin polymerization. J. Muscle Res. Cell Motil. *4*, 253–262.
64. Pollard, T.D. (1983). Measurement of rate constants for actin filament elongation in solution. Anal. Biochem. *134*, 406–412.
65. Machesky, L.M., Mullins, R.D., Higgs, H.N., Kaiser, D.A., Blanchoin, L., May, R.C., Hall, M.E., and Pollard, T.D. (1999). Scar, a WASp-related protein, activates nucleation of actin filaments by the Arp2/3 complex. Proc. Natl. Acad. Sci. USA *96*, 3739–3744.